One-Photon Mass-Analyzed Threshold Ionization Spectroscopy (MATI) of *trans*-Dichloroethylene (*trans*-$C_2H_2Cl_2$): Cation Structure Determination via Franck−Condon Fit†

Yong Jin Bae, Mina Lee, and Myung Soo Kim*

National Creative Research Initiative Center for Control of Reaction Dynamics and School of Chemistry, Seoul National University, Seoul 151-742, Korea

Received: November 3, 2005; In Final Form: January 20, 2006

One-photon mass-analyzed threshold ionization (MATI) spectrum of *trans*-$C_2H_2Cl_2$ was obtained by using vacuum ultraviolet radiation generated by four-wave mixing in Kr. The ionization energy determined from the position of the 0−0 band in the spectrum was 9.6306 ± 0.0006 eV. Ten vibrational fundamentals for the cation were identified. The spectrum also displayed abundant overtones and combinations, most of which could be assigned adequately by comparing with the quantum chemical results. It was found that channel interaction was not important for this system. The equilibrium geometry of the cation was estimated through the Franck−Condon fit.

I. Introduction

Determining the structures of gas phase molecular cations using high resolution spectroscopy is extremely difficult because of the difficulty to prepare such systems in high enough concentrations. Even though the state-of-the-art high-resolution zero kinetic energy photoelectron (ZEKE) spectroscopy[1−7] allows rotational resolution for simple molecular cations, it is very challenging at the moment to determine the accurate geometries of heavy polyatomic cations without much symmetry with this technique.

Mass-analyzed threshold ionization (MATI) spectrometry[8−10] detects molecular cations, rather than electrons in ZEKE, generated by pulsed-field ionization (PFI)[11] of neutrals prepared in high *n*, *l*, and *m* states, or so-called ZEKE states.[12] In MATI, cations generated by direct photoionization must be eliminated before PFI. Use of the spoil field[13] needed for this purpose and use of higher PFI voltage, is responsible for poorer resolution of MATI than ZEKE. On the other hand, mass selectivity[14] and capability to generate state-selected molecular ions[15,16] are the important advantages of MATI.

Evaluating Franck−Condon factors by utilizing molecular parameters available from quantum chemical calculations and comparing with the experimental intensity patterns in ZEKE/MATI spectra can be a very useful aid for definite vibrational assignment. In the usual two-photon scheme[17] for ZEKE/MATI, excitation to high Rydberg states occurs via an intermediate excited electronic state of a neutral. Then, inadequate information on the intermediate state may result in a rather poor Franck−Condon fit to the experimental data. The one-photon scheme[18,19] practiced in this laboratory, which does not require intermediate state information, is advantageous in this regard. It has been reported that a transition to a high Rydberg state converging to a low ionic state can borrow intensity from those converging to higher energy states. Hence, this channel interaction[12,20,21] is often suggested as a possible cause for a mismatch between calculated and experimental intensity distributions, even though other factors, especially inaccuracy in calculated geometries, might have been responsible.

The Franck−Condon analysis may go one step further to the estimation of the cation geometry. Namely, the cation geometry may be varied systematically in the calculation until a decent Franck−Condon fit is achieved. For example, a successful fit to the one-photon MATI spectral pattern was achieved for CH_2ClI and the cation geometry determined through the fit was reported.[22] For this approach to be successful, a requirement is that the distortion of the spectral pattern due to the channel interaction be rather insignificant.

The vibrational spectrum of *trans*-dichloroethylene cation in the ground electronic state was measured by Ng and co-workers using the pulsed field ionization-photoelectron (PFI−PE) spectroscopy.[23] Some discrepancies were observed between the experimental intensity pattern and the Franck−Condon factors evaluated using the molecular parameters calculated at the CCSD(T) level. In this work, a higher quality vibrational spectrum has been obtained with one-photon MATI. It will be shown that a decent Franck−Condon fit to the spectrum is possible by using the cation geometry which is slightly different from quantum chemical results and that the channel interaction seems to be insignificant for this system.

II. Experimental Section

trans-$C_2H_2Cl_2$ was purchased from TCI (Tokyo) and used without further purification. A gaseous sample was seeded in Ar at the stagnation pressure of 2 atm, supersonically expanded through a pulsed nozzle (diameter = 500 μm; General Valve) and introduced to the ionization chamber through a skimmer (diameter = 1 mm; Beam Dynamics) placed about 3 cm downstream from the nozzle orifice. The typical background pressure in the ionization chamber was 2×10^{-8} Torr.

The method to generate pulsed vacuum ultraviolet (VUV) radiation by four-wave difference frequency mixing in Kr was explained in detail previously[24−26] and will not be repeated here. The VUV laser pulse with the spectral bandwidth of around 1

† Part of the "Chava Lifshitz Memorial Issue".

* To whom correspondence should be addressed. E-mail: myungsoo@snu.ac.kr. Telephone: +82-2-880-6652. Fax: +82-2-889-1568.

10.1021/jp056347b CCC: $33.50
Published on Web 02/18/2006

cm^{-1} was collinearly overlapped with the molecular beam in a counterpropagation manner, and slit electrodes were used to collect the ions efficiently. Weak spoil field (1−2 V/cm) was applied to remove the directly produced ions. To achieve the pulsed-field ionization (PFI)[11] of the neutral compounds in ZEKE states, the electric field of 25V/cm was applied at 20 μs delay time after the VUV pulse. The ions generated were then accelerated, flown through a field-free region, and detected. Scrambling field[13] was applied at the laser irradiation time, which significantly lengthened the lifetime of the ZEKE states. Photoelectric current from a thin gold plate placed in the VUV beam path was used to calibrate the VUV intensity.[27] In addition, intensities of the same peak in the spectra obtained under different VUV generating conditions (different dyes in the ω_3 dye laser) were utilized for reliable calibration. The typical MATI peak width measured in this work was around 14 cm^{-1}.

III. Theoretical Outline and Computation

A. Quantum Chemical Calculation. Quantum chemical calculations were carried out for the *trans*-$C_2H_2Cl_2$ neutral and cation in the ground electronic states at various levels including the Hartree−Fock (HF), the second-order Möller−Plesset perturbation theory (MP2), and the density functional theory (DFT) using GAUSSIAN 98 suite of programs.[28] The size of the basis set was systematically increased until the basis set dependence became insignificant. Equilibrium geometries, Hessians, vibrational frequencies, and normal mode eigenvectors were obtained for the *trans*-$C_2H_2Cl_2$ neutral and cation.

B. Vibrational Selection Rule. The vibrational selection rule in ZEKE/MATI is essentially the same as that for general electronic transitions derived with the Born−Oppenheimer approximation. Neutrals under the beam condition are mostly in the ground vibrational state, which is totally symmetric (a_g in the case of *trans*-$C_2H_2Cl_2$). Then, the transitions to the totally symmetric vibrational states of the cation such as the fundamentals and overtones for totally symmetric modes, the even number overtones for nontotally symmetric modes (a_u, b_g, and b_u in the present case), and totally symmetric combinations are allowed. However, it is known that the transitions to nontotally symmetric states may appear also, even though weakly, via vibronic mechanism. Relative intensities of the electric dipole-allowed vibrational peaks can be estimated by simple Franck−Condon calculation, while those for the forbidden transitions are zero under the Born−Oppenheimer approximation.

C. Franck—Condon Factor. The method of Sharp and Rosenstock[29] which treats vibrations as harmonic was adopted to calculate the Franck−Condon factors. In this calculation, the geometries, vibrational frequencies, and normal mode eigenvectors for the initial and final states are needed. Properties of the cation were assumed to approximate those of the ion core of a high Rydberg state. The following relation was used to account for the changes in normal coordinates upon ionization.

$$\mathbf{Q}'' = \mathbf{J}\mathbf{Q}' + \mathbf{K} \tag{1}$$

Here, $\mathbf{Q}''$ and $\mathbf{Q}'$ are the normal coordinates for the neutral compound and cation in the ground states, respectively, **J** is the Duschinsky matrix representing changes in the normal mode pattern, and **K** is a matrix representing changes in the equilibrium geometry upon ionization. The internal coordinates used to calculate **J** and **K** were five bond lengths, CC, two CH, and two CCl, four bond angles, two ∠CCCl and two ∠CCH, and three dihedral angles, ∠ClCCCl, ∠HCCH, and ∠ClCCH. From **J** and **K**, the following **C** and **D** matrices were evaluated.

$$\mathbf{C} = 2\mathbf{\Gamma}'^{1/2}[\mathbf{J}^\dagger\mathbf{\Gamma}''\mathbf{J} + \mathbf{\Gamma}']^{-1}\mathbf{\Gamma}'^{1/2} - \mathbf{1} \tag{2}$$

$$\mathbf{D} = -2\mathbf{\Gamma}'^{1/2}[\mathbf{J}^\dagger\mathbf{\Gamma}''\mathbf{J} + \mathbf{\Gamma}']^{-1}\mathbf{J}^\dagger\mathbf{\Gamma}''\mathbf{K} \tag{3}$$

Here $\mathbf{\Gamma}'$ and $\mathbf{\Gamma}''$ are diagonal matrices which have the vibrational frequencies of the cation and the neutral compound, respectively, as the diagonal elements. Then, Franck−Condon factors were evaluated from **C** and **D** as follows.

$$\mathrm{FCF}(i) = D_i^2/2, \quad i\text{-mode fundamental} \tag{4}$$

$$\mathrm{FCF}(i,j) = (2C_{ij} + D_iD_j)^2/4, \quad i,j \text{ modes combination} \tag{5}$$

Even though both **J** (mode−mode coupling) and **K** (geometry change) affect **D**, the influence of the latter is more important. Hence, the geometry change upon ionization is the most important factor determining the relative intensities of fundamentals. On the other hand, both the geometry change and the mode−mode coupling affect the relative intensities of overtones and combinations.

TABLE 1: Geometries of the *trans*-$C_2H_2Cl_2$ Neutral and Cation in the Ground Electronic States Calculated at the B3LYP Level Using the 6-311++G(3df,3pd) Basis Set

	neutral ($\tilde{X}^1A_g$)		cation ($\tilde{X}^2A_u$)
C_{2h}	expt[a]	B3LYP	B3LYP[b]
	Interatomic Distance (Å)		
C═C	1.332	1.322	1.390 (0.068)
C−Cl	1.725	1.730	1.652 (−0.078)
C−H	1.092	1.079	1.084 (0.005)
	Bond Angle (deg)		
∠CCCl	120.8	121.8	120.8 (−1.0)
∠CCH	124.0	123.8	121.9 (−1.9)
	Dihedral Angle (deg)		
∠ClCCCl	180.0	180.0	180.0
∠ClCCH	0.0	0.0	0.0

[a] The experimental values by gas-phase electron diffraction in ref 31. [b] Numbers in the parentheses show the geometrical changes upon ionization between the calculated results.

IV. Results and Discussion

A. Quantum Chemical Calculation. In all the calculations performed at the HF, MP2, and DFT levels using various basis sets, the *trans*-$C_2H_2Cl_2$ neutral and cation have been found to be planar with the C_{2h} symmetry. Considering valence orbitals only, the ground-state electron configuration of the neutral compound[30] is $...(6b_u)^2(7a_g)^2(2a_u)^2$, resulting in the $\tilde{X}^1A_g$ ground electronic state. Here $2a_u$ is a π orbital with C═C bonding and C−Cl antibonding character. Both $7a_g$ and $6b_u$ correspond to the chlorine 3p in-plane nonbonding orbitals, n(Cl $3p_{\parallel}$). Removal of an electron from $2a_u$ results in the ground state of the cation, $\tilde{X}^2A_u$.

The optimized geometries of the neutral compound and the cation obtained at the B3LYP/6-311++G(3df,3pd) level are listed in Table 1 together with experimental data for the neutral compound.[31] It is seen that the calculated geometry agrees quite well with the experimental one for the neutral. Geometry changes upon ionization between the calculated results are also listed in Table 1. The C═C bond length is lengthened and the C−Cl bond lengths are shortened upon ionization in agreement with the character of the $2a_u$ orbital losing an electron. In addition ∠CCCl and ∠CCH bond angles decrease slightly.

These lead one to expect strong fundamentals and overtones for the vibrational modes with CC stretching, CCl stretching, CCCl bending, and CCH bending characters in the MATI spectrum.

trans-$C_2H_2Cl_2$ has 12 nondegenerate normal modes, $\nu_1-\nu_5$ belonging to a_g, ν_6 and ν_7 to a_u, ν_8 to b_g, and $\nu_9-\nu_{12}$ to b_u following the Mulliken notation. Calculated vibrational frequencies for the neutral compound and the cation are listed in Table 2 together with experimental data for the neutral compound.[32] For the a_g modes, ν_1 is symmetric C−H stretching, ν_2 is C═C stretching, ν_3 is symmetric CCH in-plane bending, ν_4 is symmetric C−Cl stretching, and ν_5 is symmetric CCCl in-plane bending. ν_6 and ν_7 are due to asymmetric out-of-plane bending while ν_8 is due to symmetric out-of-plane bending. For the b_u modes, ν_9 is asymmetric C−H stretching, ν_{10} is asymmetric CCH in-plane bending, ν_{11} is asymmetric C−Cl stretching, and ν_{12} is asymmetric CCCl in-plane bending. As an aid to vibrational assignment, the Franck−Condon factors for the fundamentals normalized to that of the 0−0 band have been calculated using the quantum chemical results, which are listed in the same table. The calculated Franck−Condon factors predict strong fundamentals for the $\nu_2-\nu_5$ modes in agreement with the qualitative prediction based on the geometry changes upon ionization.

B. One-Photon MATI Spectrum and Ionization Energy. One-photon MATI spectra of *trans*-$C_2H_2Cl_2$ recorded by monitoring $C_2H_2Cl_2^+$ generated in the ground electronic state are shown in Figure 1. Spectral acquisition beyond 80600 cm^{-1} could not be made because of poor VUV intensity. Intensities of the peaks in the spectrum of $C_2H_2{}^{37}Cl_2^+$ are around 10% of the corresponding peaks in the spectrum of $C_2H_2{}^{35}Cl_2^+$. Regardless, the three spectra are essentially the same except for isotopic shifts.

The most intense peak at around 77662 ± 1 cm^{-1} which moves slightly depending on the experimental condition is the 0−0 band, the position of which corresponds to the ionization energy. To determine the correct ionization energy, its position was measured using various PFI fields with the spoil field turned off and the results were extrapolated to the zero field limit. The ionization energies thus determined were 9.6306 ± 0.0006, 9.6305 ± 0.0006, and 9.6304 ± 0.0006 eV for $C_2H_2{}^{35}Cl_2$, $C_2H_2{}^{35}Cl^{37}Cl$, and $C_2H_2{}^{37}Cl_2$ isotopomers, respectively. These are in excellent agreement with the PFI−PE result reported by Ng and co-workers[23] as compared in Table 3.

C. Vibrational Assignment. Assuming that the spoil field affects positions of all the peaks appearing in the MATI spectrum similarly, the vibrational frequency of the cation corresponding to each peak can be estimated simply by taking the difference of its position from that of the 0−0 band. Vibrational frequency scale with the origin at the 0−0 band position is also shown in Figure 1. Positions and relative intensities of peaks appearing in the spectrum are listed in Table 2. Isotopic shifts for C_2H_2 $^{35}Cl^{37}Cl^+$ are also listed in the same table. It is to be mentioned that experimental isotopic shifts were compared with the calculated ones, whenever possible, to check the reliability of the assignment. Table 2 also shows the assignments for the peaks, some details of which will be described below.

Using the calculated frequencies and Franck−Condon factors, four intense peaks at 1451, 1257, 943, and 368 cm^{-1} could be readily assigned to 2^1, 3^1, 4^1, and 5^1, respectively. Referring to the calculated frequencies, two fundamentals may appear below the position of the 5^1 fundamental, namely 7^1 at 166 cm^{-1} and 12^1 at 252 cm^{-1}. In addition to the two peaks observed at 163 and 251 cm^{-1}, two additional peaks were observed, namely at 222 and 321 cm^{-1}. The latter was apparently due to the transition to the 7^2 state which is totally symmetric, while the former was found to be the 0−0 band of the cis isomer.[33] Also to be mentioned is that the width (around 7 cm^{-1}) of the 7^1 peak at 163 cm^{-1} was noticeably narrower than that of the 0−0 band and those of other fundamentals. Various experimental conditions were checked such as the VUV beam quality at this wavelength and signal saturation to find out the causes for the peak shape distortion. None could be found. We do not have any explanation for this phenomenon at the moment.

Presence of several strong fundamentals at low-frequency range means that their overtones and combinations will appear at higher frequency, complicating the identification of other fundamentals which are electric dipole-forbidden and hence are expected to be rather weak. Accordingly, all the possible overtones and combinations had to be checked before making positive identification for forbidden fundamentals, even though the results turned out to be trouble-free. Namely, the peaks at 836, 873, 1236, and 955 cm^{-1} could be positively assigned to the fundamentals 6^1, 8^1, 10^1, and 11^1, respectively.

All the vibrations showing strong fundamentals, namely ν_2, ν_4, and ν_5, displayed overtone peaks, namely 5^2 and 5^3 at 736 and 1104 cm^{-1}, respectively, 4^2 and 4^3 at 1886 and 2825 cm^{-1}, respectively, and 2^2 at 2879 cm^{-1}. Also prominent were 7^n (n = 2−5) progressions at 321, 478, 634, and 789 cm^{-1}.

Appearance of several strong fundamentals and their overtones led to many prominent combinations resulting in remarkably rich spectral feature. In fact, identification of many of these combinations rendered invaluable support to overall assignment. In searching for the combinations, not only the frequencies but also the intensities were used as guidelines. Namely, the relative intensity of a^nb^m was estimated as the product of those for a^n and b^m in the experimental spectrum and compared with that of the candidate. Among the combinations of two vibrational modes, those involving 7^n were the most abundant such as 5^17^n (n = 1−4) at 535, 696, 855, and 1013 cm^{-1}, 5^27^n (n = 1−2) at 909 and 1072 cm^{-1}. 4^17^n, 4^27^n, 3^17^n, and 2^17^n were identified also, even though some of these formed composite bands with others. Binary combinations involving $\nu_2-\nu_5$ were abundant in numbers also, such as 4^n5^m, 3^n5^m, 3^n4^m, etc. Even ternary combinations of these modes appeared, even though very weakly. Also observed were combinations involving nontotally symmetric modes. Many peaks which were expected to show measurable intensities could not be identified, however, because of the presence of stronger peaks in their very vicinity. Peaks that could be assigned are listed in Table 2.

Two peculiar aspects of ν_7 have been noted already, unusually strong fundamental considering its forbidden nature and narrower bandwidth than those of the 0−0 band and other fundamentals. Another peculiar aspect was observed in its combination with ν_5, namely negative anharmonicity.[34−37] As has been assigned already, 7^n (n = 1−5) progressions appear at 163, 321, 478, 634, and 789 cm^{-1} with a moderately positive anharmonicity. Considering that 5^1 appears at 368 cm^{-1}, one expects to observe 5^17^n (n = 1−4) at 531, 689, 846, and 1002 cm^{-1} or slightly lower considering usually positive anharmonicity. Instead, the corresponding peaks are observed at 535, 696, 855, and 1013 cm^{-1}, respectively. 5^27^n (n = 1−2) expected at 899 and 1057 cm^{-1} appear at 909 and 1072 cm^{-1}, respectively. The same trend of negative anharmonicity in 5^m7^n combinations are observed for ternary combinations involving ν_5 and ν_7 such as $4^15^17^2$, $4^15^27^1$, and $4^15^27^2$. Some cases of negative anharmonicity have been reported in the photoelectron

TABLE 2: Theoretical and Experimental (MATI) Vibrational Frequencies (in cm^{-1}), Peak Intensities, and Their Assignments for the *trans*-$C_2H_2Cl_2^+$ in the Ground Electronic State[a]

		neutral ($\tilde{X}^1A_g$)		cation ($\tilde{X}^2A_u$)				
		expt[b]	B3LYP	theor			MATI	
mode	sym	freq	freq[c]	freq[c]	int[e,f]	int[e,f]	freq	int[e]
				Fundamentals				
1	a_g	3073	3225	3189	2.49×10^{-4}	3.27×10^{-4}		
2	a_g	1578	1642	1466	0.646	0.719	1451	0.754
3	a_g	1274	1303	1279	0.341	0.153	1257	0.200
4	a_g	846	852	947 (−3)	0.332	0.451	943 (−3)	0.470
5	a_g	350	353	368 (−4)	0.897	0.806	368 (−3)	0.820
6	a_u	900	931	858			836	0.052
7	a_u	227	214	166 (−1)			163	0.081
8	b_g	763	806	885			873	0.011
9	b_u	3090	3224	3190				
10	b_u	1200	1225	1265 (−1)			1236 (−2)	0.050
11	b_u	828	815	955 (−3)			955 (−5)	0.080
12	b_u	250	240	252 (−1)			251	0.007
				Overtones and Combinations				
cis							222	0.025
7^2				332 (−2)		0.162	321 (−1)	0.162
7^3				498 (−3)			478 (−1)	0.022
$5^1 7^1$				534 (−5)			535 (−4)	0.062
7^4				664 (−4)		0.039	634 (−1)	0.024
$5^1 7^2$				700 (−6)		0.131	696 (−4)	0.143
5^2				736 (−8)		0.357	736 (−7)	0.319
7^5				830 (−5)			789 (−5)	0.006
$5^1 7^3$				866 (−7)			855 (−4)	0.022
$5^2 7^1$				902 (−9)			909 (−7)	0.021
$5^1 7^4$				1032 (−8)		0.032	1013 (−7)	0.020
cis							1032	0.015
$5^2 7^2$				1068 (−10)		0.058	1072 (−8)	0.054
$5^3+4^1 7^1$							1104	0.115
$6^1 7^2+5^1 7^5$							1160	0.010
$5^1 6^1+5^2 7^3$							1205	0.040
$4^1 5^1$				1315 (−7)		0.373	1311 (−5)	0.320
$3^1 7^1+4^1 7^3$							1420	0.030
$4^1 5^1 7^1+5^4$							1472	0.060
$5^1 6^1 7^2 + 5^2 7^5$							1532	0.010
$3^1 7^2+4^1 7^4+5^2 6^1+7^2 10^1$							1570	0.095
$2^1 7^1+5^1 10^1$							1614	0.035
$3^1 5^1$				1647 (−4)		0.136	1624 (−2)	0.128
$4^1 5^1 7^2$				1647 (−9)		0.060	1637 (−5)	0.070
$4^1 5^2$				1683 (−11)		0.169	1679 (−10)	0.175
$2^1 7^2 +4^1 6^1$							1772	0.132
$2^1 5^1$				1834 (−4)		0.610	1816 (−5)	0.610
$4^1 5^2 7^1$				1849 (−12)			1852 (−6)	0.035
4^2				1894 (−6)		0.130	1886 (−1)	0.100
$4^1 11^1+4^1 5^2 7^2+3^1 7^4$							1903	0.045
$2^1 7^3+5^1 7^2 10^1$							1931	0.028
$3^1 5^1 7^2$				1979 (−6)		0.022	1951 (−5)	0.025
$5^2 10^1+2^1 5^1 7^1$							1979	0.030
$3^1 5^2$				2015 (−8)		0.066	1992 (−8)	0.040
$4^1 5^2 7^2$				2015 (−13)		0.027	2013 (−11)	0.030
$4^1 5^3+4^2 7^1$							2047	0.060
$2^1 7^4+3^1 6^1$							2090	0.023
$2^1 5^1 7^2+4^1 5^1 6^1$							2143	0.145
$2^1 5^2$				2202 (−8)		0.282	2181 (−8)	0.240
$3^1 4^1+4^1 10^1$							2197	0.115
cis							2223	0.020
$4^2 5^1$				2262 (−10)		0.109	2254 (−10)	0.080
$2^1 5^1 7^3 + 5^2 7^2 10^1$							2299	0.020
$3^1 5^3$				2383 (−12)		0.028	2356 (−7)	0.020
$2^1 4^1$				2413 (−3)		0.362	2391 (−3)	0.373
$2^1 5^1 7^4 + 3^1 5^1 6^1$							2456	0.042
$2^1 5^2 7^2+3^1 4^1 7^2+4^2 7^4+4^1 7^2 10^1+3^2+4^1 5^2 6^1$							2513	0.090
$2^1 5^3+2^1 4^1 7^1+4^1 5^1 10^1$							2547	0.083
$3^1 4^1 5^1$				2594 (−7)		0.064	2565 (−5)	0.070
$4^2 5^2$				2630 (−14)		0.050	2622 (−11)	0.065
$2^1 5^1 6^1+4^1 5^1 11^1$							2639	0.033
$2^1 10^1+2^1 5^2 7^3$							2669	0.023
$2^1 3^1+2^1 4^1 7^2$						0.140	2699	0.160
$2^1 4^1 5^1$				2781 (−7)		0.312	2754 (−4)	0.245
$4^3+2^1 5^2 7^4+3^1 5^2 6^1$							2825	0.019
2^2				2932		0.245	2879	0.190

[a] Numbers in parentheses are isotopic shifts for $C_2H_2{}^{35}Cl^{37}Cl^+$. [b] IR/Raman spectroscopic data in ref 32. [c] B3LYP/6-311++G(3df,3pd) results. [d] Intensities calculated with molecular parameters obtained at the B3LYP/6-311++G(3df,3pd) level. [e] Normalized to that of the 0−0 band. [f] Determined via Franck−Condon fit. See text for details.

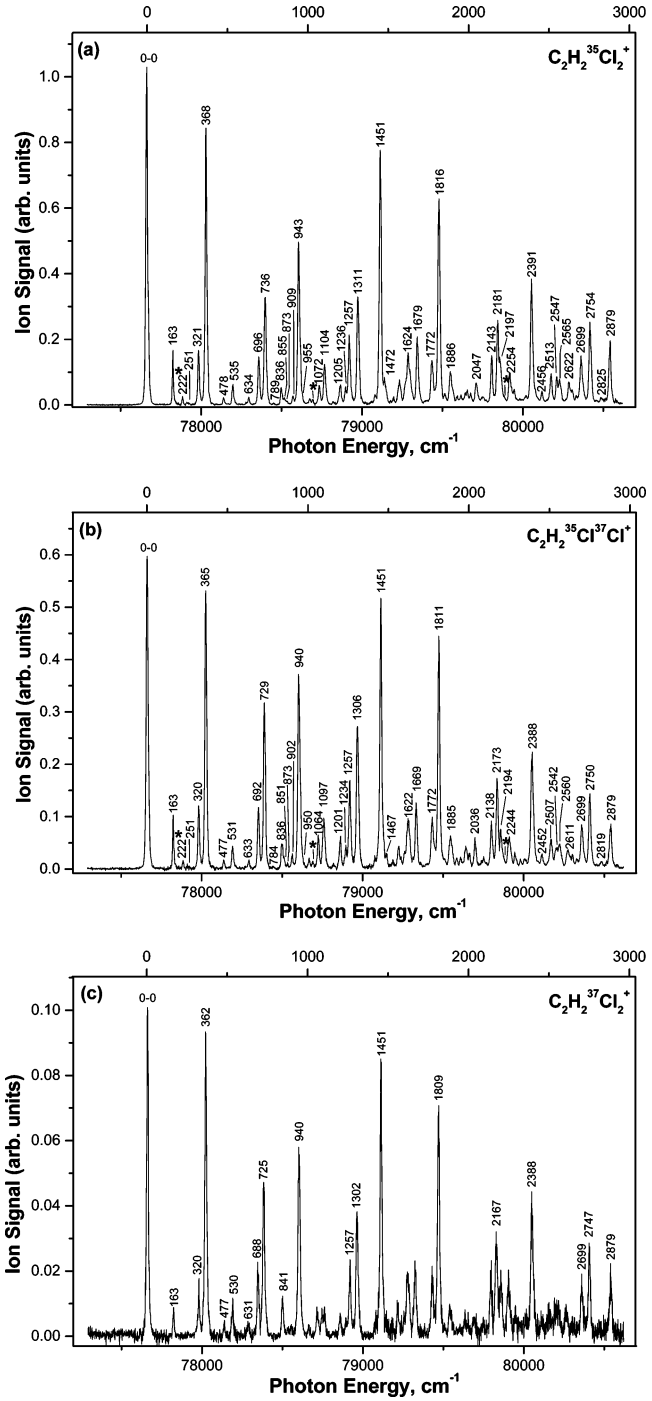

Figure 1. One-photon MATI spectra of *trans*-$C_2H_2Cl_2$ recorded by monitoring trans isomers of (a) $C_2H_2{}^{35}Cl_2{}^+$, (b) $C_2H_2{}^{35}Cl^{37}Cl^+$, and (c) $C_2H_2{}^{37}Cl_2{}^+$ in the ground electronic state. The *x*-scale at the top of the figure corresponds to the vibrational frequency scale for the cation in cm^{-1}. Its origin is at the 0−0 band position. Stars indicate peaks due to the cis isomer.

TABLE 3: Ionization Energy (IE) to the Ground Electronic State of *trans*-$C_2H_2Cl_2$ Cation, in eV

	IE($\tilde{X}$)	
trans-$C_2H_2{}^{35}Cl_2$	9.6306 ± 0.0006	this work
trans-$C_2H_2{}^{35}Cl^{37}Cl$	9.6305 ± 0.0006	this work
trans-$C_2H_2{}^{37}Cl_2$	9.6304 ± 0.0006	this work
trans-$C_2H_2Cl_2$	9.63097 ± 0.00025	ref 23
trans-$C_2H_2Cl_2$	9.65 ± 0.02	ref 39

spectroscopic studies of simple molecular cations.[38] Since the negative anharmonicity is observed only for the combinations involving ν_5 and ν_7 in this work, mode−mode coupling between these vibrations may be responsible for this phenomenon. Its details are beyond the scope of the present work, however. Also, it is not clear at the moment whether the suspected mode−mode coupling is responsible for the peculiarities of the ν_7 system mentioned above.

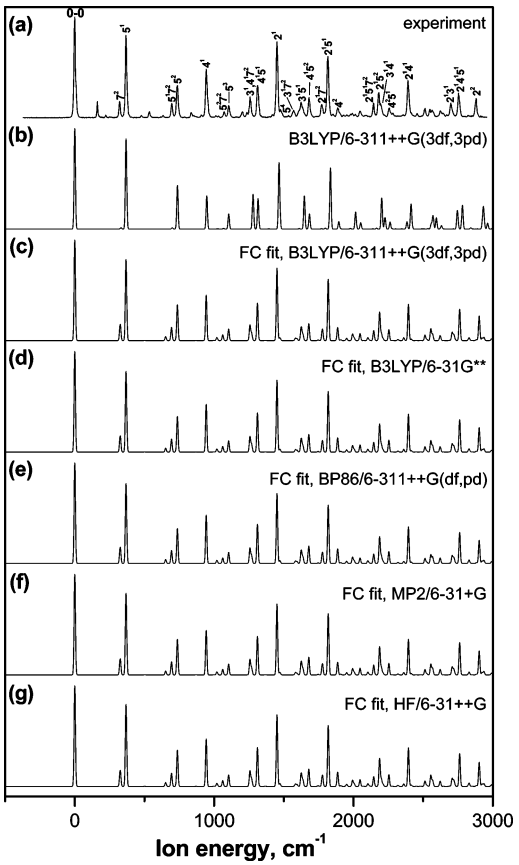

Figure 2. (a) One-photon MATI spectrum of *trans*-$C_2H_2Cl_2$. (b) A spectrum simulated by using the Franck−Condon factors calculated with the molecular parameters obtained at the B3LYP/6-311++G(3df,3pd). The simulated spectra obtained via Franck−Condon fit (see text for details) using experimental data and eigenvectors calculated at the B3LYP/6-311++G(3df,3pd), B3LYP/6-31G**, BP86/6-311++G(df,pd), MP2/6-31+G, and HF/6-31++G are shown in parts c−g, respectively.

D. Franck—Condon Fit. Appearance of abundant overtones and combinations in the MATI spectrum of *trans*-$C_2H_2Cl_2$ makes it an ideal system to check the importance of the channel interaction[12,20,21] and the applicability of the Franck−Condon fit in determining the structures of gas phase polyatomic cations. Simply speaking, if the intensities of some low-frequency peaks including the 0−0 band in the experimental spectrum are significantly larger than the calculated results even after the best effort to fit, interference from the channel interaction must be suspected. On the other hand, it may be safely ignored if the intensities of almost all the electric dipole-allowed fundamentals, overtones, and combinations in the low-frequency region can be reproduced by Franck−Condon calculations.

As an initial attempt, the Franck−Condon factors were calculated using the geometries, vibrational frequencies, and eigenvectors of the *trans*-$C_2H_2Cl_2$ neutral and cation obtained by quantum chemical calculations and the spectrum was simulated by taking into account the experimental bandwidth (14 cm^{-1}). The simulated spectrum obtained by using the parameters from the calculations at the B3LYP/6-311++G(3df,3pd) level, Figure 2b, is compared with the experimental spectrum, Figure 2a. Number of peaks appearing

in the simulated spectrum is much less than that in the experimental one mainly because only the peaks due to the transitions to the totally symmetric vibrational states are present in the former. Even after taking into account such a difference, it is apparent that the former is not a good quantitative representation of the latter. The most noticeable difference is near absence of the 7^2 peak at 321 cm^{-1}. In addition, the calculated 5^1, 5^2, and 3^1 peaks are stronger while those of 4^1 and 2^1 are weaker than experimental ones. Particularly conspicuous is the intensity reversal of the 5^2 and 4^1 peaks at 736 and 943 cm^{-1}, respectively, in the two spectra. On the basis of the stronger intensity of 7^2 in the experimental spectrum, one may argue that the channel interaction between the Rydberg states converging to the 7^2 vibrational state of the cation and those to higher energy vibrational states might have caused strengthening of this peak. Inspecting the two spectra carefully, however, one finds that all the combinations involving 7^2, such as 5^17^2, 5^27^2, 2^17^2, etc., display stronger signals in the experimental spectrum. On the other hand, the overtones and combinations involving 5^n and 3^n, other than those involving 7^n also, are weaker in the experimental spectrum. These suggest that the mismatch between the experimental and calculated intensity patterns are not due to the channel interaction but probably due to the inaccuracy of the molecular parameters used in the calculation, which were obtained by quantum chemical calculation.

For rigorous comparison between the experimental and calculated intensity patterns, it is necessary to calculate Franck−Condon factors by using experimental molecular parameters, or accurate ground-state potential energy surfaces both for the neutral compound and for the cation. The ground-state geometry and the vibrational frequencies of the *trans*-$C_2H_2Cl_2$ neutral are available in the literature,[31,32] while the vibrational frequencies of the cation have been determined in this work. Accurate normal mode eigenvectors are difficult to get. Hence, those of the neutral compound and the cation obtained by quantum chemical calculations were used. Finally, the cation geometrical parameters were treated as variables and were changed systematically attempting to achieve a good fit between the experimental and calculated spectral patterns in the low-frequency region. Calculated data were used for the C−H bond lengths because the C−H stretching peaks were not observed and hence changing them was meaningless. Even after the best attempt to fit, the experimental intensity of 7^2, and those of the other totally symmetric overtones and combinations involving ν_7 also, could not be reproduced adequately through calculations. As an attempt to reproduce the intensity of 7^2, the C_{77} element of the **C** matrix in eq 2 was varied, arriving at a good fit at C_{77} of 0.569. Then, the intensities of the other totally symmetric overtones and combinations involving ν_7 became similar to the experimental results also. The simulated spectrum thus obtained using the eigenvectors obtained at the B3LYP/6-311++G(3df,3pd) level is shown as Figure 2c. It is to be noted that the intensity pattern in this spectrum resembles the experimental almost even to the minor details. In particular, the relative intensities of the peaks mentioned above such as those involving 3^n, 4^n, 5^n, and 7^n are well reproduced by simulation. Also, the intensity reversal between the 5^2 and 4^1 peaks no longer occurs. Finally, it is to be mentioned that the intensities of prominent peaks at high-frequency region were reproduced quite well even though the fit was made using the low-frequency peaks mostly. This means that the harmonic approximation made in the method of Sharp and Rosenstock[29] is adequate in the present case. Intensities of major peaks calculated here are listed in Table 2 and compared with the experimental ones.

TABLE 4: Equilibrium Geometries[a] Obtained by Using Quantum Chemical Calculation and Franck−Condon Fit

level	basis set	C═C	C−Cl	CCCl	CCH
	Quantum Chemical Calculation[b]				
B3LYP	6-311++G(3df,3pd)	1.390	1.652	120.8	121.9
B3LYP	6-31G**	1.397	1.665	120.8	122.2
BP86	6-311++G(df,pd)	1.392	1.670	120.6	122.5
MP2	6-31+G	1.400	1.723	120.9	123.3
HF	6-31++G	1.390	1.712	121.5	122.0
	av	1.394	1.684	120.9	122.4
	std dev	±0.004	±0.031	±0.3	±0.6
	Franck−Condon Fit[c]				
B3LYP	6-311++G(3df,3pd)	1.394	1.642	120.8	120.2
B3LYP	6-31G**	1.393	1.641	121.0	120.0
BP86	6-311++G(df,pd)	1.393	1.642	121.0	120.1
MP2	6-31+G	1.390	1.639	121.4	119.7
HF	6-31++G	1.394	1.638	121.4	120.4
	av	1.393	1.640	121.1	120.1
	std dev	±0.002	±0.002	±0.3	±0.3

[a] Bond lengths in Å and bond angles in degree. [b] Equilibrium geometries determined by direct quantum chemical optimization. [c] Equilibrium geometries determined via Franck−Condon fit to the MATI spectrum using eigenvectors obtained at various quantum chemical levels.

Even though a good fit has been achieved, two weaknesses in the present approach are evident. One is the necessity of using the calculated eigenvectors and the other is arbitrary change of an element of the **C** matrix. Even though the former looks inevitable, some validation seems to be needed for the latter. Instead, we carried out similar calculations using the eigenvectors obtained at various quantum chemical levels and basis sets but using the same value for the C_{77} as determined above. When the eigenvectors obtained at the B3LYP and BP86 levels were used, good fits were achieved regardless of the basis sets used in the quantum chemical calculation. The equilibrium geometries thus optimized were very similar also, bond lengths within ±0.002 Å and bond angles within ±0.3°. Use of the eigenvectors obtained at the MP2 and HF levels resulted in good fits as shown in Figure 2 even though the equilibrium geometries thus optimized were slightly different from those optimized by using the eigenvectors obtained at the DFT levels. The optimized equilibrium geometries obtained using eigenvectors calculated at some typical levels are listed in Table 4. Also listed in the table are the equilibrium geometries obtained by straightforward quantum chemical optimization at the corresponding levels. It is to be noticed that the bond lengths and bond angles optimized by the present scheme are nearly the same regardless of the quantum chemical levels used to obtain the eigenvectors while those obtained by direct quantum chemical optimization show much larger scatter. Namely, even though C_{77} was adjusted arbitrarily, the results are consistent. For example, the C═C bond length calculated at various quantum chemical levels listed in Table 4 is scattered in the 1.390−1.400 Å range while the scatter is less in present results, 1.390−1.394 Å. For the C−Cl bond length, difference in the scatter is more dramatic, 1.652−1.723 vs 1.638−1.642 Å. More importantly, use of the calculated eigenvectors, which is inevitable, looks acceptable as far as the final results are concerned. It is thought that the cation geometry determined via Franck−Condon fit in this work can be regarded as a benchmark in the test of improved or newly developed quantum chemical methods.

V. Summary and Conclusion

Interference by channel interaction at the time of excitation to high Rydberg states is one of the outstanding issues in the field of ZEKE/MATI spectroscopy. In its absence, the structure of a polyatomic cation may be estimated rather reliably through the Franck−Condon analysis of the vibrational intensity pattern. One-photon MATI spectrum of *trans*-$C_2H_2Cl_2$ measured in this work displayed many prominent vibrational fundamentals, overtones, and combinations, which makes it a good system to check the importance of the channel interaction. The spectrum simulated with the Franck−Condon factors calculated with the molecular parameters obtained from quantum chemical results did not agree with the experimental one quantitatively. However, careful inspection indicated that erroneous molecular parameters, not the channel interaction, were mainly responsible for the mismatch. A scheme has been devised to improve the Franck−Condon fit, namely by using experimental geometry and frequencies for the neutral compound, experimental frequency for the cation, calculated eigenvectors for the neutral compound and the cation and treating the cation geometry as the adjustable parameters. Using this scheme, successful fits to the experimental spectrum could be achieved even to the minor details. Also, level-to-level variation in the optimized geometry was not significant. The results suggest that the channel interaction is not important for the present system at least. Finally, it is to be mentioned that the present scheme can be useful to determine the geometry of a gas-phase polyatomic cation, which has been much sought after but is difficult to get at the moment. However, further tests with other systems are needed to establish this as a useful structural probe.

Acknowledgment. This work was financially supported by CRI, Ministry of Science and Technology, Republic of Korea. Y.J.B. and M.L. thank the Ministry of Education for the Brain Korea 21 fellowship.

References and Notes

(1) Sommavilla, M.; Merkt, F. *J. Phys. Chem. A* **2004**, *108*, 9970.
(2) Ford, M. S.; Tong, X.; Dessant, C. E. H.; Müller-Dethlefs, K. *J. Chem. Phys.* **2003**, *119*, 12914.
(3) Signorell, R.; Merkt, F. *J. Chem. Phys.* **1999**, *110*, 2309.
(4) Seiler, R.; Hollenstein, U.; Softley, T. P.; Merkt, F. *J. Chem. Phys.* **2003**, *118*, 10024.
(5) Hollenstein, U.; Seiler, R.; Schmutz, H.; Andrist, M.; Merkt, F. *J. Chem. Phys.* **2001**, *115*, 5461.
(6) Liu, J.; Hochlaf, M.; Chambaud, G.; Rosmus, P.; Ng, C. Y. *J. Phys. Chem. A* **2001**, *105*, 2183.
(7) Hochlaf, M.; Baer, T.; Qian, X. M.; Ng, C. Y. *J. Chem. Phys.* **2005**, *123*, 144302.
(8) Lee, M.; Kim, H.; Lee, Y. S.; Kim, M. S. *J. Chem. Phys.* **2005**, *123*, 024310.
(9) Kwon, C. H.; Kim, H. L.; Kim, M. S. *J. Phys. Chem. A* **2003**, *107*, 10969.
(10) Georgiev, S.; Chakraborty, T.; Neusser, H. J. *J. Phys. Chem. A* **2004**, *108*, 3304.
(11) Ng, C. Y. *Annu. Rev. Phys. Chem.* **2002**, *53*, 101.
(12) Schlag, E. W. *ZEKE Spectroscopy*; Cambridge University Press: Cambridge, U.K., 1998.
(13) Park, S. T.; Kim, H. L.; Kim, M. S. *Bull. Korean Chem. Soc.* **2002**, *23*, 1247.
(14) Zhu, L.; Johnson, P. *J. Chem. Phys.* **1991**, *94*, 5769.
(15) Park, S. T.; Kim, S. K.; Kim, M. S. *Nature* **2002**, *415*, 306.
(16) Park, S. T.; Kim, M. S. *J. Am. Chem. Soc.* **2002**, *124*, 7614.
(17) Xie, Y.; Su, H.; Tzeng, W. B. *Chem. Phys. Lett.* **2004**, *394*, 182.
(18) Kwon, C. H.; Kim, M. S. *J. Chem. Phys.* **2004**, *121*, 2622.
(19) Lee, M.; Kim, M. S. *J. Phys. Chem. A* **2003**, *107*, 11401.
(20) Chupka, W. A.; Grant, E. R. *J. Phys. Chem. A* **1999**, *103*, 6127.
(21) Yeretzian, C.; Hermann, R. H.; Ungar, H.; Selzle, H. L.; Schlag, E. W.; Lin, S. H. *Chem. Phys. Lett.* **1995**, *239*, 61.
(22) Lee, M.; Kim, H.; Lee, Y. S.; Kim, M. S. *J. Chem. Phys.* **2005**, *122*, 244319.
(23) Woo, H. K.; Wang, P.; Lau, K. C.; Xing, X.; Ng, C. Y. *J. Phys. Chem. A* **2004**, *108*, 9637.
(24) Park, S. T.; Kim, S. K.; Kim, M. S. *J. Chem. Phys.* **2001**, *114*, 5568.
(25) Kwon, C. H.; Kim, H. L.; Kim, M. S. *J. Chem. Phys.* **2003**, *118*, 6327.
(26) Kwon, C. H.; Kim, H. L.; Kim, M. S. *J. Chem. Phys.* **2003**, *119*, 215.
(27) Samson, J. A. R. *Techniques of Vacuum Ultraviolet Spectroscopy*; Wiley: New York, 1967.
(28) Frisch, M. J.; Trucks, G. W.; Schlegel, H. B.; et al. *Gaussian 98*, revision A.6. Gaussian Inc.: Pittsburgh, PA, 1998.
(29) Sharp, R. E.; Rosenstock, H. M. *J. Chem. Phys.* **1964**, *41*, 3453.
(30) Takeshita, K. *J. Chem. Phys.* **1999**, *110*, 6792.
(31) Schäfer, L.; Ewbank, J. D.; Siam, K.; Paul, D. W.; Monts, D. L. *J. Mol. Struct.* **1986**, *145*, 135.
(32) Shimanouchi, T. *Tables of Molecular Vibrational Frequencies Consolidated Volume I*; National Bureau of Standards: Washington, DC, 1972.
(33) Bae, Y. J.; Lee, M.; Kim, M. S. Unpublished results.
(34) Eland, J. H. D. *Photoelectron Spectroscopy 2nd ed.*; Butterworth Press: London, 1984.
(35) Pivonka, N. L.; Kaposta, C.; Helden, G.; Meijer. G.; Wöste, L.; Neumark, D. M.; Asmis, K. R. *J. Chem. Phys.* **2002**, *117*, 6493.
(36) Thompson, W. E.; Marilyn, E. J. *J. Chem. Phys.* **2001**, *114*, 4846.
(37) Silverstone, H. J.; Harrell, E.; Grot, C. *Phys. Rev. A* **1981**, *24*, 1925.
(38) Eisenhardt, C. G.; Baumgärtel, H. *Ber. Bunsen-Ges. Phys. Chem.* **1998**, *102*, 1803.
(39) Lias, S. G.; Bartmess, J. E.; Liebman, J. F.; Levin, R. D.; Mallard, W. G. *J. Phys. Chem. Ref. Data* **1988**, *17*, Supplement No. 1.